A COMBINATORIAL DESCRIPTION OF SOME HEEGAARD FLOER HOMOLOGIES

SUCHARIT SARKAR AND JIAJUN WANG

Abstract. In this paper, we give an algorithm to compute the hat version of the Heegaard Floer homology of a 3-manifold. This method also allows us to compute the filtrations coming from a knot in a 3-manifold.

1. Introduction

Heegaard Floer homology is a 3-manifold invariant introduced by Peter Ozsváth and Zoltán Szabó [3]. There are four versions, denoted by $\widehat{HF}, HF^\infty, HF^+$ and HF^-, which are graded abelian groups satisfying certain long exact sequences. A knot K in a 3-manifold Y induces a filtration of $\widehat{CF}(Y)$, and the filtration type is a knot invariant. The successive quotients give a knot invariant $\widehat{HFK}(K,Y)$, which was discovered independently by Ozsváth-Szabó [4] and Jacob Rasmussen [6]. This invariant, called the knot Floer homology, is a categorification of Alexander polynomial for knots in S^3, and among other things, it detects fiberedness, the genus of a knot, and there is an invariant τ coming from the knot filtration whose absolute value gives a lower bound for the slice genus.

All these invariants are constructed after taking a Heegaard diagram of the 3-manifold Y with some basepoint w (and another basepoint z in case we are considering knots in Y). The differentials count the number of points in certain moduli spaces, which are hard to describe in general. People were interested to find a combinatorial description of these theories, or equivalently, an algorithm to compute these invariants.

In this paper, we give such an algorithm to compute $\widehat{HF}(Y)$ for a 3-manifold Y, and also the ordinary knot Floer homology of a knot in any 3-manifold. All our computations will be done with coefficients in $\mathbb{F}_2$. We shall be trying to find a nice Heegaard diagram satisfying certain properties, and with such Heegaard diagrams it will be easy to compute some of the Heegaard Floer homologies.

It will be interesting to compare our paper with the recent work of Ciprian Manolescu, Peter Ozsváth and the first author in [2], where they give a combinatorial description of knot Floer homology of knots in S^3.

We remark that we do not know whether this method can be generalized to compute some of the other versions, notably $HF^\infty(Y)$ and $HF^+(Y)$.

The paper is organized as follows. In Section 2, we give an algorithm to get a nice Heegaard diagram. In Section 3, we give a combinatorial characterization of (pseudo) holomorphic disks missing the basepoint w in such Heegaard diagrams. In Section 4, we give examples to demonstrate our algorithm on knots in S^3 and on 3-manifolds.

Acknowledgement. The first author wishes to thank Zoltán Szabó for introducing him to the subject of Heegaard Floer homology and having many helpful discussions at various points. He also wishes to thank Matthew Hedden and Robert Lipshitz for their comments.

1991 *Mathematics Subject Classification.* Primary 57R58.

Key words and phrases. Heegaard Floer homology; knot Floer homology.

This work was done when the second author is an exchange graduate student in Columbia University. He is grateful to the Columbia math department for its hospitality. He also would like to thank Rob Kirby and Peter Ozsváth for their continuous guidance, support and encouragement.

We would like to thank Ciprian Manolescu, Peter Ozsváth and Dylan Thurston for pointing out mistakes, making comments and having helpful discussions during the developement of this work. An argument in Subcase 4.2 was suggested by Dylan Thurston.

2. Nice Heegaard diagrams

In this section, we demonstrate an algorithm which, starting with an admissible pointed Heegaard diagram, isotopes and handleslides the β curves to get an admissible Heegaard diagram which has only bigon and square regions other than the one containing the basepoint.

For a Heegaard diagram, a connected component of the complement of α and β curves is called a region. A disk region is a $2n$-gon if its boundary contains n α edges. A periodic domain is a linear combination of regions whose boundary is a linear combination of some full α circles and β circles. A Heegaard diagram is admissible if any periodic domain has both positive and negative coefficients.

We call bigon and square regions *good* and all other regions *bad*.

2.1. **Killing non-disk regions.** Let $\mathcal{H}$ be an admissible Heegaard diagram. Note that the complement of the α curves is a punctured sphere. So any region is either a disk or a (punctured) annulus. A non-disk region D has more than one boundary components, and each of them must have both α edges and β edges since $\mathcal{H}$ is admissible. Then we could make a finger move on the β curve to reduce the number of boundary components of D without generating other non-disk regions. See Figure 1 for this finger move operation. Repeating this process as many times as necessary, we will kill all non-disk regions.

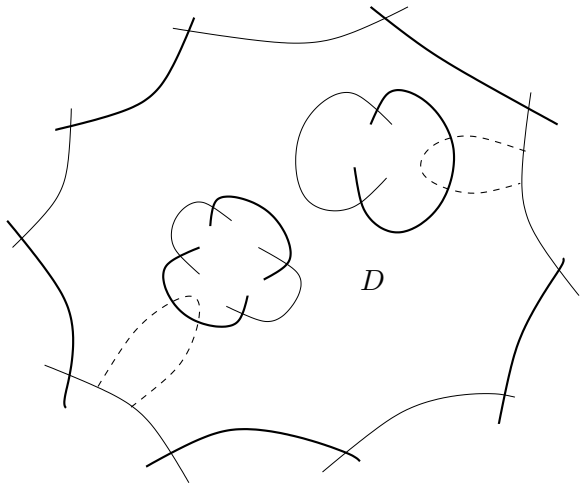

Figure 1. **Killing non-disk regions**
Here, the thicker lines are α curves, the thinner lines are β curves, and the dotted lines are fingers. After our finger move, the region D becomes a disk region.

2.2. **Making all but one regions bigons or squares.** In this subsection, we just consider Heegaard diagrams with only disk regions. Note that our algorithm will not generate non-disk regions.

Let D_0 be the disk region containing the basepoint w. For any region D, pick an interior point w_1, define the *distance* of D, denoted by $d(D)$, to be the smallest number of intersection points of an arc (disjoint from α curves) connecting w_0 and w_1, with the β curves. For a $2n$-gon disk region D, define the *badness* of D to be $b(D) = max\{n-2, 0\}$.

For a pointed Heegaard Diagram $\mathcal{H}$ with only disk regions, define the *distance* $d(\mathcal{H})$ of $\mathcal{H}$ to be the largest distance of bad regions. Define the *distance d complexity* of $\mathcal{H}$ to be tuple

$$c_d(\mathcal{H}) = \left(\sum_{i=1}^{m} b(D_i), -b(D_1), -b(D_2), \cdots, -b(D_m)\right),$$

where $D_1, \cdots, D_m$ are all the distance d bad regions, ordered so that $b(D_1) \geq b(D_2) \geq \cdots \geq b(D_m)$. We call the first term the *total badness of distance d* of $\mathcal{H}$, and denote by $b_d(\mathcal{H})$. If there are no distance d bad regions, then $c_d(\mathcal{H}) = (0)$. We order the set of distance d complexities lexicographically.

Lemma 2.1. *For a distance d pointed Heegaard diagram $\mathcal{H}$ with only disk regions, if $c_d(\mathcal{H}) \neq (0)$, we could modify $\mathcal{H}$ by isotopies and handleslides to get a new Heegaard diagram $\mathcal{H}'$ with only disk regions, and with $d(\mathcal{H}') \leq d(\mathcal{H})$ and $c_d(\mathcal{H}') < c_d(\mathcal{H})$.*

Proof. We order the bad regions of distance d as in the definition of the distance d complexity. Now we look at D_m. It is a $(2n)$-gon with $n \geq 3$. Pick an adjacent region D_* with distance $d-1$ having a common β edge with D_m. Let b_* be (one of) their common β edge(s). We order the α edges of D_m counterclockwise, and denote them by $a_1, a_2, \cdots, a_n$.

We try to make a finger move on b_* into the D_m and out of D_m through a_2, as indicated in Figure 2 when D_m is an octogan. Our finger will separate D_m into two parts, $D_{m,1}$ and $D_{m,2}$.

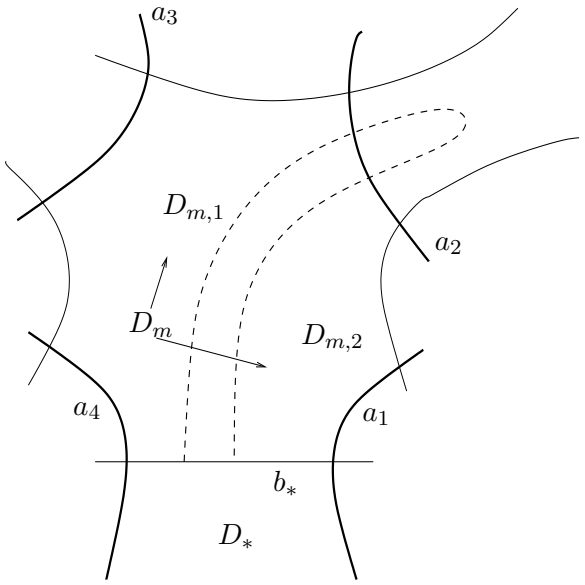

FIGURE 2. **Starting our finger move**

If we reach a square region of distance $\geq d$, we push up our finger outside the region via the opposite edge, as in Figure 3.

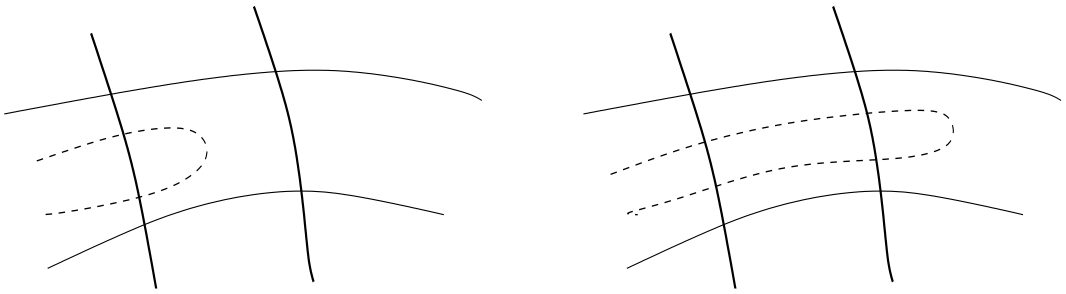

FIGURE 3. **Moving across a square region**

We continue to push up our finger as far as possible, until we reach one of the following:

(1) a bigon region.
(2) a region with distance $\leq d-1$.
(3) a bad region with distance d other than D, i.e., D_i with $i < m$.
(4) D_m.

We will prove our lemma case by case.

Case 1. A bigon is reached.

Before we reach the bigon region, all regions in between are square regions with distance $\geq d$. And after our finger moves inside a bigon region, our finger separates the bigon into a square and a new bigon. See Figure 4.

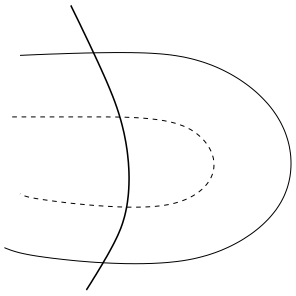

FIGURE 4. **Case 1. A bigon is reached**

Denote the new Heegaard diagram by $\mathcal{H}'$. We have $b(D_{m,1}) = b(D_m) - 1$. Since $D_{m,2}$ is a square and is good, we get $b_d(\mathcal{H}') = b_d(\mathcal{H}) - 1$. Note that we will not increase the distance of any distance d bad region since we do not pass any region of distance $\leq d-1$. So $d(\mathcal{H}') \leq d(\mathcal{H})$ and $c_d(\mathcal{H}') < c_d(\mathcal{H})$.

Case 2. A smaller distance region is reached.

Let D' be the region with distance $< d$ we reached by our finger. Suppose $d(D') = d'$. Let $\mathcal{H}'$ be the new Heegaard diagram. See Figure 5. Note that D' might be a bigon, which could be covered in both Case 1 and Case 2.

We have $b(D_{m,1}) = b(D_m) - 1$ and $D_{m,2}$ is good. Our finger separates D' in to a bigon region D'_1 and the other part D'_2. When D' is a square or a bad region, D'_2 will be a bad region of distance $d' < d$. Certainly we have increased the distance d' complexity. But we have $d(\mathcal{H}') \leq d(\mathcal{H})$ and $c_d(\mathcal{H}') < c_d(\mathcal{H})$.

Case 3. Another distance d bad region is reached.

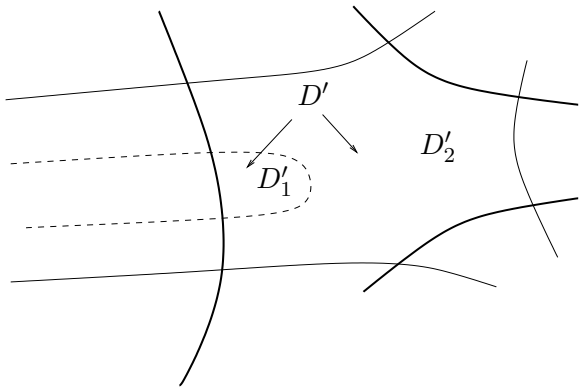

FIGURE 5. **Case 2. A smaller distance region is reached.**

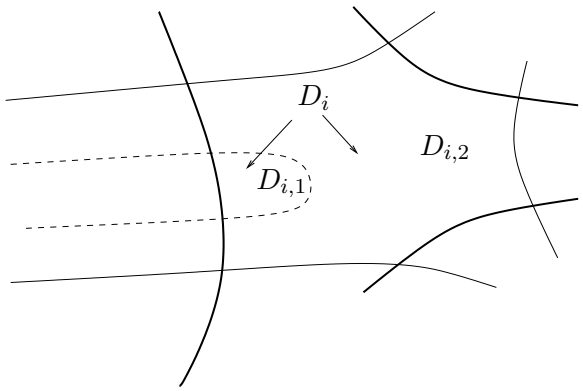

FIGURE 6. **Case 3. Another distance d bad region is reached.**

In this case, we reach some distance d bad region D_i with $i < m$. See Figure 6 for an indication. Denote by $D_{i,1}$ and $D_{i,2}$ the two parts of D_i separated by our finger. Then $D_{i,1}$ is good while $D_{i,2}$ is a bad region of distance d. We have $b(D_{i,2}) = b(D_i) + 1$ and $b(D_{m,1}) = b(D_m) - 1$. So the total badness of distance d remains the same. But we are decreasing the distance d complexity since we are moving the badness from a later bad region to an earlier bad region. So for the new Heegaard diagram $\mathcal{H}'$, we have $d(\mathcal{H}') = d(\mathcal{H})$ and $c_d(\mathcal{H}') < c_d(\mathcal{H})$.

Case 4. Coming back to D_m. This is the worst case and we need to pay more attention. We divide this case into two subcases.

Subcase 4.1. Coming back via an adjacent region.

This subcase is indicated in Figure 7.

In this case, we see the full copy of some β curve, say β_i, along our long finger. Suppose $b_* \subset \beta_j$. Note that $i \neq j$. Now instead of doing finger move, we handleslide β_j over β_i. This is indicated in Figure 8.

Note that after the handle slides, we are not increasing the distance of any bad region. We have increased the badness of D_*, but it is a distance $d-1$ region. $D_{m,2}$ is a bigon region and $b(D_{m,1}) = b(D_m) - 1$. So for the new Heegaard diagram $\mathcal{H}'$ after the handleslide, the total badness of distance d is decreased by 1. We have $d(\mathcal{H}') \leq d(\mathcal{H})$ and $c_d(\mathcal{H}') < c_d(\mathcal{H})$.

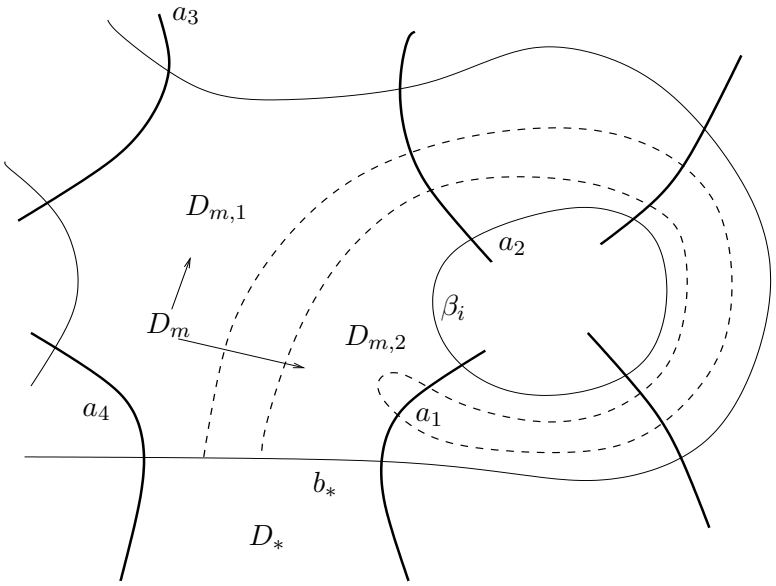

FIGURE 7. **Case 4.1 Coming back via an adjacent edge - finger move**

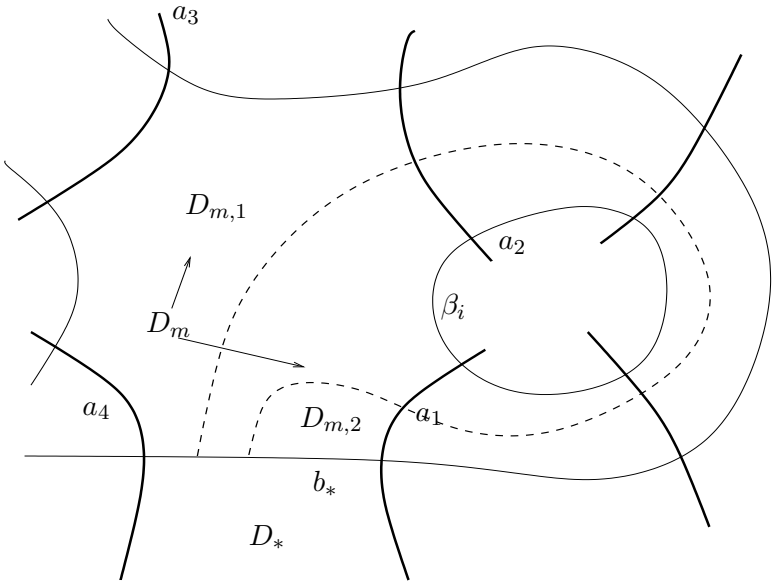

FIGURE 8. **Case 4.1 & 4.2 Coming back via an adjacent edge - handleslide**

Subcase 4.2. Coming back via a non-adjacent edge.

If we return through a_k with $3 < k \leq n$.Then, instead of the finger move through a_2, we do a finger move through a_3 (starting from b_*). If we reach one of the first three cases, we are decreasing the distance d complexity by similar arguments as before.

Suppose instead that we are coming back, say via a_i. We claim that $3 < i < k$. Certainly we can not come back via a_3 or a_k. If $i > k$ or $i < 3$, we could close the cores the two fingers to get two simple closed curves c_1 and c_2. Then c_1 and c_2 intersect transversely at exactly one point and they are in the complement of the beta curves. The complement of the beta

curves is a punctured sphere. Attach disks to get a sphere. Then as homology classes, we get $[c_1] \cdot [c_2] = 1$. But $H_1(S^2) \cong \{1\}$. This is a contradiction. So we must have $3 < i < k$. (The argument of this claim is suggested by Dylan Thurston.)

Now we do another finger move through a_4. And contiue the same arguments. We either end up with a finger which does not come back, or we get some finger that starts at a_j and coming back via a_{j+1}. For a finger not coming back, we reduce to previous cases and the lemma follows.

For a finger starting at a_j and coming back at a_{j+1}, we see a full β circle. We do a handleslide as in Subcase 4.1. We have $b(D_{m,1}) = \max\{n - j - 1, 0\}$ and $b(D_{m,2}) = \max\{j - 2, 0\}$. And $b(D_{m,1}) + b(D_{m,2}) \leq n - 2$. So for the new Heegaard diagram $\mathcal{H}'$ after the handleslide, the total badness of distance d decreases. We have $d(\mathcal{H}') \leq d(\mathcal{H})$ and $c_d(\mathcal{H}') < c_d(\mathcal{H})$.

And we end the proof of our lemma.

□

Repeat this process to make $c_d = (0)$. And further repeating this process will eventually kill all bad regions other than D_0.

2.3. **Admissibility.** In this subsection, we show that our algorithm will not change the admissibility. There are two operations involved in our algorithm: isotopies and handleslides.

The isotopy is the operation in Figure 9.

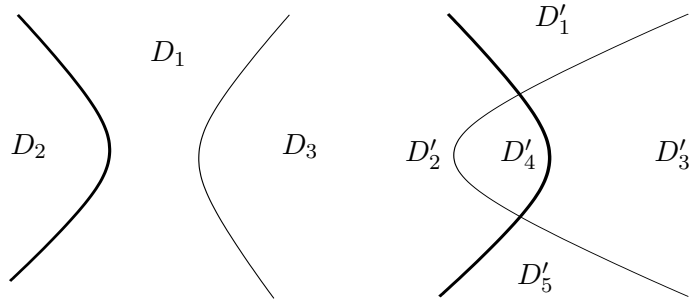

FIGURE 9. **Isotopy of the β curve**

Let $\mathcal{H}$ and $\mathcal{H}'$ be the Heegaard diagrams before and after the isotopy. Suppose $\mathcal{H}$ is admissible. For a periodic domain in $\mathcal{H}'$

$$\phi' = c_1 D_1' + c_2 D_2' + c_3 D_3' + c_4 D_4' + c_5 D_5' + \cdots$$

we have $c_2 - c_1 = c_4 - c_3 = c_2 - c_5$ and $c_1 - c_3 = c_2 - c_4 = c_5 - c_3$. Hence $c_1 = c_5$ and $c_4 = c_2 + c_3 - c_1$. Note that the regions are all the same except those in Figure 9. So

$$\phi = c_1 D_1 + c_2 D_2 + c_3 D_3 + \cdots$$

is a periodic domain for $\mathcal{H}$. Since $\mathcal{H}$ is admissible, ϕ has both positive and negative coefficients, and so does ϕ'. Hence $\mathcal{H}'$ is admissible.

Our handleslide is the one in Figure 10.

Let us make notations of the regions as indicated in Figure 10. Suppose $\mathcal{H}$ is admissible. For a periodic domain in $\mathcal{H}'$

$$\phi' = c_* D_*' + c_1 D_{m,1}' + c_2 D_{m,2}' + c_{1,1} S_{1,1}' + c_{1,2} S_{1,2}' + \cdots + c_{k,1} S_{k,1}' + c_{k,2} S_{k,2}' + \cdots$$

We will get $c_1 - c_* = c_{1,1} - c_{1,2} = \cdots = c_{k,1} - c_{k,2} = c_2 - c_*$. Suppose $c_1 - c_* = c_0$, then $c_{i,1} = c_{i,2} + c_0$ and $c_1 = c_2$. Now

$$\phi = c_* D_* + c_1 D_m + c_{1,1} S_1 + \cdots + c_{k,1} S_k + \cdots$$

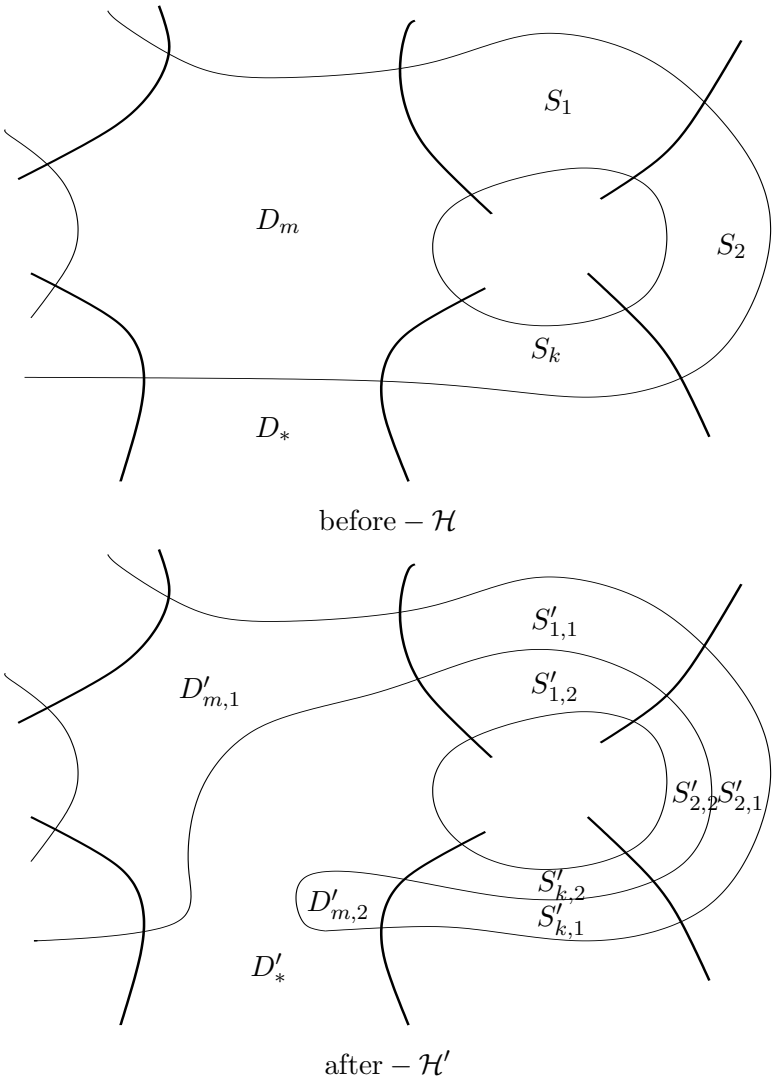

FIGURE 10. **Handleslide of the β curve**

is a periodic domain for $\mathcal{H}$. Since $\mathcal{H}$ is admissible, we get that ϕ, and hence ϕ', has both positive and negative coefficients. So $\mathcal{H}'$ is admissible.

2.4. **Summary.** Thus, starting with an admissible pointed Heegaard diagram, our algorithm gives an admissible Heegaard diagram with only one bad region, a $2n$-gon containing the basepoint w.

We have similar conclusions for links in 3-manifolds. In fact, an admissible Heegaard diagram for a link with k components in 3-manifold has $2k$ basepoints, $w_1, \cdots, w_k$ and $z_1, \cdots, z_k$. For any $i \neq j$, w_i and w_j are separated by some α curve. Our algorithm could be modified to get an admissible Heegaard diagram such that every region containing no w points is a good region. Note that every region is connected to exactly one region containing some w point in the complement of the α curves, so we can define the distance and hence the complexity in the same way, and thus our algorithm works as before.

We call such a Heegaard diagram **nice**.

3. Holomorphic disks

Given a Heegaard diagram, we may suppose that the genus $g > 2$ by stabilization if necessary. Then by Section 2, we can get a nice Heegaard diagram with basepoint $w \in D_0$.

Let $\phi \in \pi_2(x, y)$. As $g > 2$, this is equivalent to an expression $D(\phi) = \sum_i a_i D_i$. Actually with a different formulation of $\pi_2(x, y)$, this equivalence holds even for $g = 2$. Let $Mas(\phi) = 1$. We assume that ϕ does not pass through w, i.e. $a_0 = 0$. If we have $(k-1)$ extra α circles and k basepoints $w_1, w_2, \cdots w_k$ with $w_i \in D_{0,i}$, we shall assume $a_{0,i} = 0$. We want to count the number of (unparametrized) holomorphic representatives of ϕ.

We can choose a complex structure on $Sym^g(\Sigma_g)$, close to the one coming from Σ_g, such that, whenever any $a_i < 0$, ϕ has no holomorphic representative. So now, in addition, assume $a_i \geq 0 \forall i$.

Theorem 3.1. *Under these conditions, ϕ has a unique holomorphic representative.*

Proof. By Lipshitz' formula [1], $Mas(\phi) = e(\phi) + \mu_x + \mu_y$, and $e(\phi) = \sum_i a_i e(D_i) \geq 0$ as $e(D_i) \geq 0$ since D_i is either a bigon or a square. Thus $0 \leq \mu_x + \mu_y \leq 1$.

Now let $x = (x_1, x_2, \ldots, x_g)$ and $y = (y_1, y_2, \ldots, y_g)$, with $x_i, y_i \in \alpha_i$. Since ϕ is non-trivial, it has to hit at least one α circle, say α_1 and hence (as $\partial(\partial\phi_{|\alpha}) = y - x$), $\mu_{x_1}, \mu_{y_1} \geq \frac{1}{4}$. (When we say ϕ hits some α circle, we mean $\partial\phi$ is non-zero on some part of that α circle).

We now note that $e(\phi)$ can only take half-integral values, and thus only the following cases might occur.

- ϕ hits α_1 and α_2, $D(\phi)$ consists of squares, $\mu_{x_1} = \mu_{x_2} = \mu_{y_1} = \mu_{y_2} = \frac{1}{4}$
- ϕ hits α_1, $D(\phi)$ consists of squares, $\mu_{x_1} + \mu_{y_1} = 1$
- ϕ hits α_1, $D(\phi)$ consists of squares and exactly one bigon, $\mu_{x_1} = \mu_{y_1} = \frac{1}{4}$

The first case corresponds to a map from F to Σ, where F is a connected double branched cover over D^2 with 0 Euler characteristic and 1 double point (for holomorphic maps, the number of double points is given by $\mu_x + \mu_y - e(\phi)$), i.e. F is a square.

The map induces a complex structure on F (with 4 marked points on the boundary), and hence there is a unique holomorphic branched cover $F \to D^2$ satisfying boundary conditions, and upto reparametrization (assuming the count doesn't change as we slightly perturb our complex structure).

The other cases corrospond to maps from a single cover of D^2 (i.e. from D^2) to Σ. Hence the second case can not occur, because number of double points has to be 0 and in this case we have number of double points = 1(2).

In the last case, the map from D^2 to Σ induces a complex structure on D^2 and 2 marked points on the boundary, and hence there is a unique holomorphic map to the standard D^2, after reparametrization (again after assuming the perturbation condition holds). □

To complete the previous theorem, we need to show that when we perturb our complex structures a little, the count does not change. This property holds, if the map from F to Σ is an embedding. So now we try to analyse $D(\phi)$ as a whole, and not just the individual regions. In the first case, $D(\phi)$ is an immersed square tiled by squares, which is an embedding near the 4 corners, and in the last case $D(\phi)$ is an immersed bigon tiled by squares and 1 bigon, which is also an embedding near its 2 corners.

Theorem 3.2. *With conditions as above, $D(\phi)$ is an embedded square or embedded bigon, even when extended to the boundary.*

Proof. We shall be concentrating on the case of the square in more details, but the other case is similar.

Case 1. In this case we have an immersion $f : F \to \Sigma$, where F is a square (with boundary). Look at the preimage of all the α and β circles in F (and by abuse of notation, we shall also be calling them α and β arcs). Using the embedding condition near the 4 corners, we see that at each corner only one α arc and only one β arc can come in. The different α arcs cannot intersect and the different β arcs cannot intersect, and all intersections between α and β arcs are transverse.

Note that since the preimage of each square region is a square, so F (with all the α and β arcs) is also tiled by squares. Thus in F there cannot be any closed loop, for then $F\backslash\{$inside of loop$\}$ has e negative and hence cannot be tiled by squares. Also no α arc can enter and leave F through the same β arc on the boundary, for again the outside will have negative e. Thus the α arcs slice up F into vertical rectangles, and in each rectangle, no β arc can enter and leave through the same α arc. This shows that the α arcs and β arcs make the standard co-ordinate chart on F.

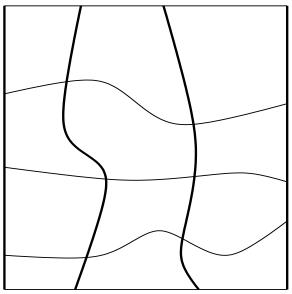

FIGURE 11. **Preimage of α and β arcs for a square**

We call the intersection points between α and β arcs as vertices (and we shall be calling the 4 original vertices of the square F as corners). Note that to show f is an embedding, it is enough to show that no 2 different vertices map to the same point. Assume $p, q \in F$ be distinct vertices with $f(p) = f(q)$. There could be 2 subcases.

- Both p and q are in $\mathring{F}$.
- At least one of p and q is in ∂F.

We shall be reducing the first subcase to the second. So assume both are in the interior of F. Choose a direction on the α arc passing through $f(p) = f(q)$ in Σ, and keep looking at successive points of intersection with β arcs, and locate their inverse images in F. For each point, we shall get at least a pair of inverse images, one on the α arc through p, and one on the α arc through q, until one of the points falls on ∂F, and thus the reduction the second subcase.

In this subcase, without loss of generality, we assume that p lies on a β arc in ∂F. Then choose a direction on the β arc in Σ through $f(p) = f(q)$ and proceed as above, until one of the preimages hits an α arc on ∂F. If that preimage is on the β arc through q, then reverse the direction and proceed again, and this time we can ensure that the preimage which hits α arc on ∂F first is the one that was on the β arc through p. Thus we get 2 distinct vertices in F mapping to the same point in Σ, one of them being a corner. This is a contradiction to the embedding assumption near the corners.

Case 2. In this case we have $f : F \to \Sigma$ an immersion with F being a bigon. Again look at the preimage of α and β circles. All intesections will be transverse (call them vertices), and at each of the 2 corners there can be only one α arc and only one β arc. Again there cannot be any closed loops. We get an induced tiling on F with squares and 1 bigon.

But this time the α arcs can (in fact they have to) enter and leave F through the same β arc, but they do have to do it in a completely nested fashion (i.e. there is only one innermost bigon). Thus F decomposes into two pieces, one bigon, and one square (possibly degenerate). From the earlier case, β arcs must cut up the square piece in a standard way, and from the previous argument, the β arcs must enter and leave the bigon in a nested fashion.

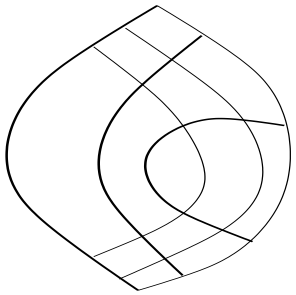

FIGURE 12. **Preimage of α and β arcs for a bigon**

Again to show f is an embedding, enough to show that it is an embedding restriced to vertices. Take 2 distinct vertices p, q mapping to the same point, and follow them along α arcs in some direction, until one of them hits a β arc on ∂F. Then follow them along β arcs, and $\exists$ some direction such that one of them will actually hit a corner, giving the required contradiction.

So in either case, f is an embedding. □

4. Examples

In this section, we give two examples to demonstrate our algorithm. One is on knot Floer homology and the other is on the Heegaard Floer homology of 3-manifolds.

4.1. **The Trefoil.** We start with the Heegaard diagram in Figure 13, where the two circles are the α curves and are identified to get a genus one Heegaard diagram.

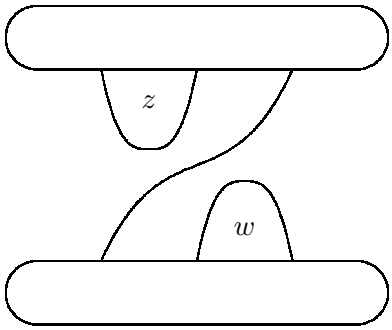

FIGURE 13. **A Heegaard diagram for the trefoil knot**

After isotopy using the algorithm in Section 2, we end up with the Heegaard diagram as in Figure 14.

So we have nine generators, as labeled in Figure 14. It is routine to find all boundary holomorphic disks and determine the Alexander and Maslov gradings of each generator.

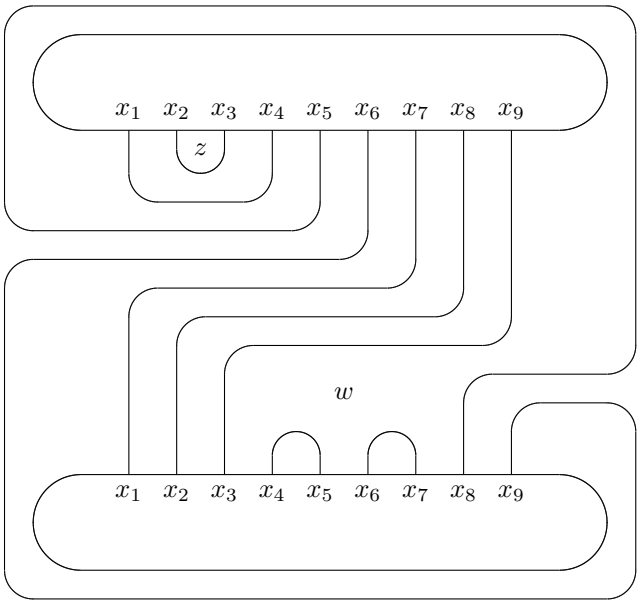

FIGURE 14. **A nice Heegaard diagram for the trefoil knot**

4.2. **The Poincaré homology sphere $\Sigma(2,3,5)$.** We start with the Heegaard diagram of $\Sigma(2,3,5)$ in Figure 15, viewed as the $+1$ surgery on the right-handed trefoil knot.

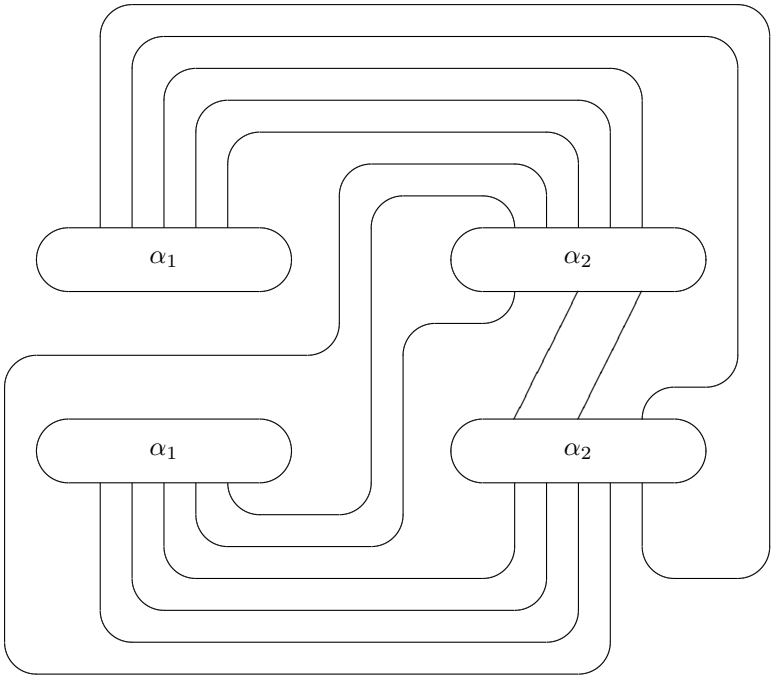

FIGURE 15. **A Heegaard diagram for the Poincaré homology sphere**

After applying our algorithm, we get a nice Heegaard diagram as in Figure 16. The dotted marked points in the diagram are those on the boundary of the region containing the base point w. We leave the actual computation using this diagram to the patient reader.

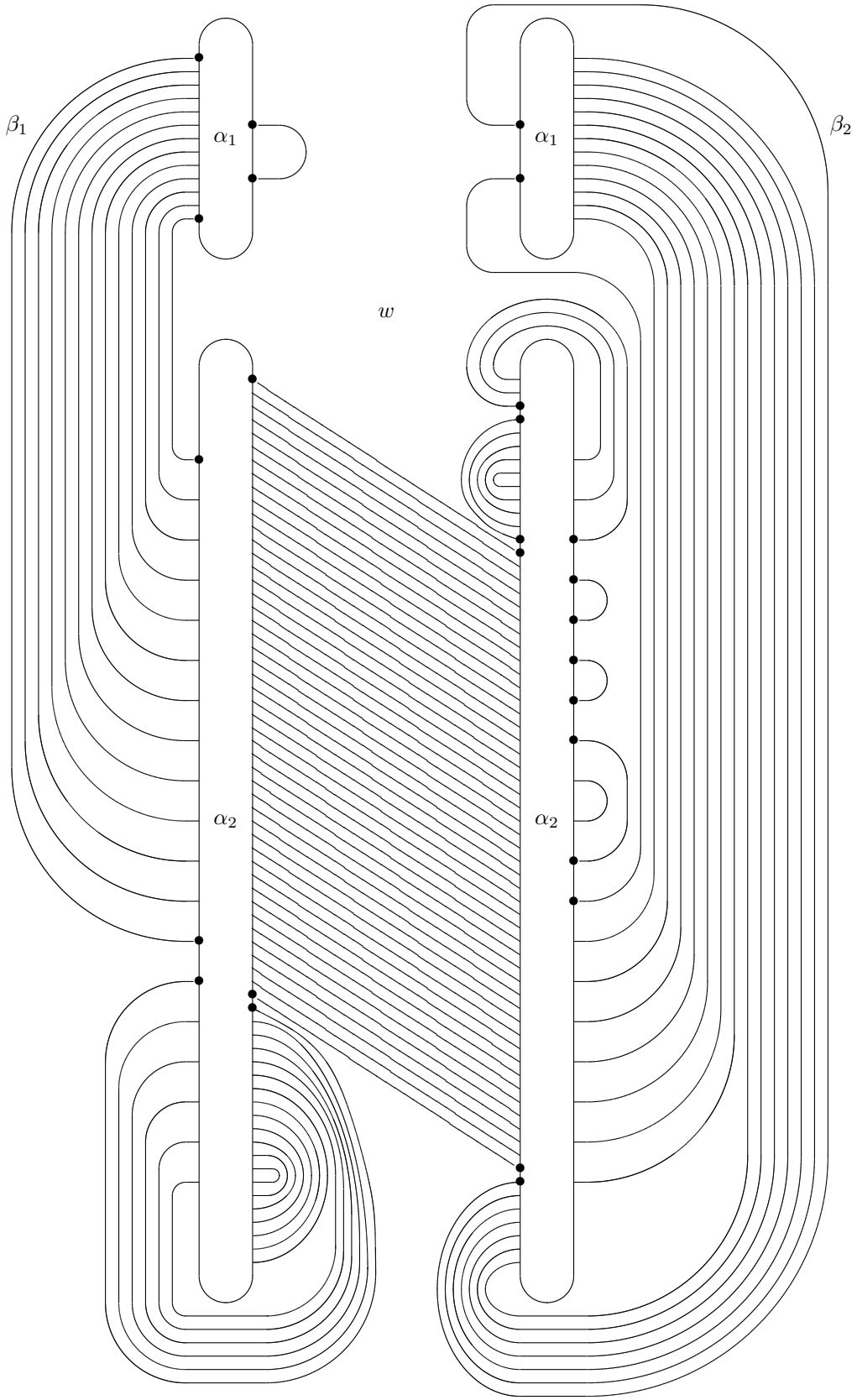

FIGURE 16. **A nice Heegaard diagram for the Poincaré homology sphere**

References

[1] R. Lipshitz. A Cylindrical Reformulation of Heegaard Floer Homology. math.SG/0502404.
[2] C. Manolescu, P. Ozsváth and S. Sarkar. A combinatorial description of knot Fler homology. math.GT/0607691.
[3] P. Ozsváth and Z. Szabó. Holomorphic disks and topological invariants for closed three-manifolds. *Ann. of Math. (2)*, 159(3):1159–1245, 2004.
[4] P. Ozsváth and Z. Szabó. Holomorphic disks and knot invariants. *Adv. Math.*, 186(1):58–116, 2004.
[5] P. Ozsváth and Z. Szabó. Heegaard diagrams and Floer homology. To appear in *the Proceedings for ICM-2006 Madrid*.
[6] J. Rasmussen. Floer homology and knot complements. Ph.D Thesis, Harvard Univ., 2003.

Department of Mathematics, Princeton University, Princeton, NJ 08544
sucharit@math.princeton.edu

Department of Mathematics, UC Berkeley, Berkeley, CA 94720
wang@math.berkeley.edu